HHS Public Access

Author manuscript

Macromol Chem Phys. Author manuscript; available in PMC 2017 July 12.

Published in final edited form as:

Macromol Chem Phys. 2015 April ; 216(8): 856–872. doi:10.1002/macp.201400506.

Visible-Light Initiated Free-Radical/Cationic Ring-Opening Hybrid Photopolymerization of Methacrylate/Epoxy: Polymerization Kinetics, Crosslinking Structure, and Dynamic Mechanical Properties

Dr. Xueping Ge,
Bioengineering Research Center, School of Engineering, University of Kansas, Lawrence 66045, KS, USA

Dr. Qiang Ye,
Bioengineering Research Center, School of Engineering, University of Kansas, Lawrence 66045, KS, USA

Dr. Linyong Song,
Bioengineering Research Center, School of Engineering, University of Kansas, Lawrence 66045, KS, USA

Prof. Anil Misra, and
Bioengineering Research Center, School of Engineering, University of Kansas, Lawrence 66045, KS, USADepartment of Civil Engineering, University of Kansas, Lawrence 66045, KS, USA

Prof. Paulette Spencer
Bioengineering Research Center, School of Engineering, University of Kansas, Lawrence 66045, KS, USADepartment of Mechanical Engineering, University of Kansas, Lawrence 66045, KS, USA

Abstract

The effects of polymerization kinetics and chemical miscibility on the crosslinking structure and mechanical properties of polymers cured by visible-light initiated free-radical/cationic ring-opening hybrid photopolymerization are determined. A three-component initiator system is used and the monomer system contains methacrylates and epoxides. The photopolymerization kinetics is monitored in situ by Fourier transform infrared-attenuated total reflectance. The crosslinking structure is studied by modulated differential scanning calorimetry and dynamic mechanical analysis. X-ray microcomputed tomography is used to evaluate microphase separation. The mechanical properties of polymers formed by hybrid formed by free-radical polymerization. These investigations mark the first time that the benefits of the chain transfer reaction between epoxy and hydroxyl groups of methacrylate, on the crosslinking network and microphase separation during hybrid visible-light initiated photopolymerization, have been determined.

Correspondence to: Qiang Ye; Paulette Spencer.

Supporting Information

Supporting Information is available from the Wiley Online Library or from the author.

Note: Figure 8B was corrected on April 16, 2015.

Graphical abstract

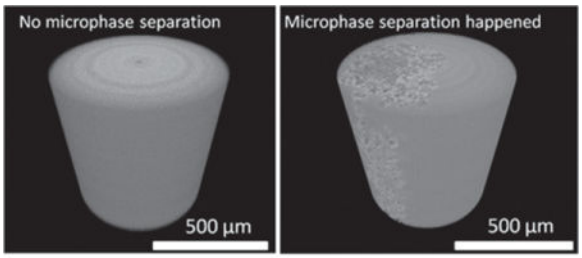

Micro-CT images of polymers

Keywords

chain transfer reaction; chemical miscibility; crosslinking structure; dynamical mechanical property; free-radical/cationic ring-opening hybrid polymerization; photopolymerization; polymerization kinetics

1. Introduction

The development of hybrid polymers is a major trend in polymer materials science.[1,2] These hybrid polymers generally exhibit excellent physical and mechanical properties as well as chemical resistance. One approach for producing hybrid polymer structures is blending two types of monomers and polymerizing by two independent mechanisms. This approach offers the potential for additional control over the polymerization kinetics as well as the structure and properties of the final material.[3] One such method is the free-radical/cationic hybrid polymerization system, which has led to the preparation of a variety of unusual hybrid polymer structures, such as block,[4–7] graft,[8,9] random copolymers[10–12] and interpenetrating polymer networks (IPNs).[13] In these hybrid systems, the order of the reactions can be controlled by the selective addition of inhibitors of each polymerization type or through manipulation of the wavelength-initiator combination. To date, the relationship between the kinetics of the free-radical/cationic hybrid polymerization and the structure/properties of the polymer cured by these hybrid systems has not been fully elucidated.[14] A better understanding of these hybrid systems would enable their purposeful formulation for widespread use throughout the polymerization industry.

Photopolymerization has been widely used in coating, inks and adhesives because of its efficiency, economy, energy savings, and environmental friendliness.[15–19] The monomer mixtures used in the free-radical/cationic hybrid photopolymerization usually contain two main types of monomers,[20–26] e.g., acrylates and epoxides/vinyl ethers. The acrylates, which undergo free-radical polymerization, exhibit high reaction rates and offer a large selection of monomers and initiators. The epoxides and vinyl ethers, which undergo cationic polymerization, do not suffer from oxygen inhibition and exhibit low toxicity and shrinkage.[27–31]

Hybrid photopolymerization has been investigated by several research teams. The use of a methacrylate/vinyl ether system to facilitate UV-initiated hybrid photopolymerization has been studied by Stansbury and colleagues.[32] A methacrylate/epoxide system has been

studied under UV curing conditions by Lecamp and coauthors.[33] By combining methacrylate and siloxane-epoxy groups into one molecule, Ortiz et al. developed monomers which could undergo free-radical/cationic ring-opening polymerization under UV-induced photopolymerization.[34] Jessop and coauthors investigated the water-chain-transfer and the effect of oxygen in acrylate/epoxide hybrid photopolymerization under UV radiation.[35,36] Chen and Cook[37] and Nowers and Narasimhan[38] studied preparation of IPN networks formed by thermally initiated cationic epoxy polymerization and UV-photocured free-radical acrylate polymerization. Nearly all of the reports have used separate radical and cationic photoinitiators, and most of the research has focused on the UV initiating system, not the visible light-induced system.

Because of the damaging effects of UV radiation, biological applications, such as dental restorations and polymer scaffolds for tissue engineering, frequently employ visible-light photoinitiator systems.[39,40] Cationic ring-opening visible-light initiated photopolymerization has been widely reported, but most of the reports focused on free-radical promoted cationic ring-opening polymerization. For example, Crivello and colleagues reported that the efficiency of cationic ring-opening polymerization of epoxides can be improved by the free-radical promoted cationic mechanism under visible light.[41,42] A series of photoinitiators were also investigated for the cationic ring-opening polymerization under visible light by Crivello's group.[43] Bi and Neckers systematically studied the three-component visible light initiator system and the free-radical promoted cationic ring-opening mechanism for epoxy monomers.[44] Recently, Lalevee et al. reported that silane can be used to accelerate radical promoted cationic ring-opening polymerization and that the overall efficiency is strongly affected by the structure of silane.[45–48]

To date, there is only one published report regarding the free-radical/cationic ring-opening hybrid photopolymerization under visible light. Oxman et al. evaluated the visible light initiator system (camphorquinone (CQ) containing three-component initiator system) used in the free-radical/cationic hybrid photopolymerization.[49] In this study, nine different electron donors were investigated, but the report provided limited information on the polymerization kinetics and crosslinking structures.

Typically, in the hybrid polymerization system, free-radical and cationic polymerization occur simultaneously to form an IPN.[1,2] IPNs often exhibit varying degrees of phase separation, which depend principally on the polymerization kinetics of the components and the miscibility of the polymers.[33,38] The rate of cationic polymerization is much lower than that of free-radical polymerization. Thus in the hybrid system, the difference in polymerization kinetics will influence the structure and properties of the IPNs.[3,13]

Understanding the polymerization kinetics and the degree of phase separation becomes important in engineering the final material properties to meet the requirements for a particular application. Research on the kinetics and the structure of the IPNs for the free-radical/cationic ring-opening hybrid polymerization system is quite limited. Moreover, the miscibility of the polymers could also influence phase separation during the formation of the IPNs.[37,50,51]

In this paper, we studied the complex polymerization kinetics and crosslinking structures formed by free-radical/cationic ring-opening hybrid photopolymerization under visible light. A three-component initiator system was used, and the monomer system contained methacrylates and epoxides. The effects of initiator concentration and monomer concentration on the polymerization kinetics were systematically studied by Fourier transform IR-attenuated total reflectance (FTIR-ATR). The acceleration effect for cationic ring-opening polymerization was also investigated. The crosslinking structures were studied by modulated differential scanning calorimetry (DSC), and the microphase separation was examined by X-ray microcomputed tomography (Micro CT). In addition to studying the effect of polymerization kinetics on the crosslinking structure, the chemical miscibility of the polymers was also considered by employing two kinds of epoxides (siloxane epoxy and oxocarbon epoxy, respectively). Based on the results, it is hypothesized that the chain transfer reaction between epoxy and hydroxyl groups in methacrylates plays an important role in the formation of the crosslinking network. To our knowledge, this is the first time that polymerization kinetics, chemical miscibility, and the chain transfer reaction have been studied in a crosslinked polymer cured by visible-light initiated free-radical/cationic ring-opening hybrid photopolymerization.

2. Experimental Section

2.1. Materials

The chemical structures are shown in Table 1. 2,2-Bis[4-(2-hydroxy-3-methacryloxypropoxy) phenyl]-propane (BisGMA, Polysciences, Warrington, PA) and 2-hydroxyethylmethacrylate (HEMA, Acros Organics, NJ) were used as received without further purification, as monomers for free radical polymerization. Two epoxy monomers (E1 and E2) were used for cationic ring-opening polymerization. CQ, ethyl-4-(dimethylamino) benzoate (EDMAB) and (4-octyloxyphenyl) phenyliodonium hexafluoroantimonate (OPPIH) were used as a three-component-photoinitiator system. CQ and EDMAB were obtained from Aldrich (Milwaukee, WI, USA). OPPIH was obtained from Gelest, Inc (Morrisville, PA). 2-(dimethylamino) ethyl methacrylate (DMAEMA, Aldrich) was used as a comparison to EDMAB. E1, a siloxane epoxy, was synthesized in our lab using a method similar to previous publications (Supporting Information).[52–54] 3,4-Epoxycyclohexylmethyl (E2), 1,1,3,3-tetramethyl disiloxane, 4-vinyl-1-cyclohexene (1,2-epoxide, mixture of isomers), tris (triphenylphosphine) rhodium(I) chloride (Wilkinson catalyst), anhydrous magnesium sulfate ($MgSO_4$), glyoxal bis (diallyl acetal) (GBDA), and all other chemicals were purchased from Sigma-Aldrich at the reagent grade and used without further purification.

2.2. Preparation of Adhesive Formulations

The preparation of the adhesive formulations has been reported.[19,55] As shown in Table 2, the control adhesive formulation (C0) consisted of HEMA and BisGMA with a mass ratio of 45/55, which is similar to widely used commercial dentin adhesives. This control was used as a comparison to the experimental adhesive resins (E1-*x* or E2-*x*) with a methacrylate/epoxy = $(100 - x)/x$ (w/w) ratio. The methacrylate in the experimental formulations was HEMA/BisGMA = 45/55 (Table 2). A three component initiator system was used containing

CQ, EDMAB (DMAEMA was also used as a comparison) and OPPIH. The concentration of initiators is shown in Table 2. All of the resin mixtures were miscible. The resin mixtures were prepared in brown glass vials; the resins were mixed for 2 days to form clear homogeneous solutions.

The experimental samples identified as E1-25 and E1-50, were also formulated with 10 wt% GBDA (glyoxal bis(diallyl acetal)) to examine the cationic ring-opening acceleration effects (Table 2 : E1-25-10 and E1-50-10). The concentration of GBDA was based on the total final weight of the adhesive resin.

2.3. Real-Time Conversion and Maximal Polymerization Rate

Real-time in situ monitoring of the visible-light-induced photopoly merization of the adhesive formulations was performed using an infrared spectrometer (Spectrum 400 Fourier transform infrared spectrophotometer, Perkin-Elmer, Waltham, MA) at a resolution of 4 cm^{-1}.[56–59] One drop of adhesive solution was placed on the diamond crystal top-plate of an ATR accessory (Pike, GladiATR, Pike Technology, Madison, WI) and covered with a mylar film. A 40-s-exposure to the commercial visible-light polymerization unit (Spectrum 800, Dentsply, Milford, DE, ≈480–490 nm,[60] at an intensity of 550 mW cm^{-2}, was initiated after 50 spectra had been recorded. Real-time IR spectra were recorded continuously for 600 s after light curing began. A time-resolved spectrum collector (Spectrum TimeBase, Perkin-Elmer) was used for continuous and automatic collection of spectra during polymerization. Three replicates were obtained for each adhesive formulation.

The change of the band ratio profile (1637 cm^{-1} (C=C)/1608 cm^{-1}(phenyl)) was monitored for calibrating the degree of conversion (DC) of the methacrylate groups. DC was calculated using the following equation, which is based on the decrease in the absorption intensity band ratios before and after light curing. The average of the last 50 values of time-based data is reported as the DC at 10 min.

$$DC = \left(1 - \frac{\text{Absorbance}^{\text{sample}}_{1637cm^{-1}} / \text{Absorbance}^{\text{sample}}_{1608cm^{-1}}}{\text{Absorbance}^{\text{monomer}}_{1637cm^{-1}} / \text{Absorbance}^{\text{monomer}}_{1608cm^{-1}}}\right) \times 100\%$$

In the hybrid system, there is a second type of reaction, i.e., epoxy ring-opening reaction. A similar method, as described above, was used to calculate the DC of the ring-opening reaction. The difference is the band ratio profile used for DC calculation. For the monomer of E1 (siloxane epoxy), the band ratio profile of (884 cm^{-1}(epoxy)/1251 cm^{-1}(Si–C)) was monitored. Overlapping spectral features made it more difficult to use the band ratio to calculate the DC of the epoxy ring-opening reaction for the monomer of E2 (oxocarbon epoxy). The decrease in the absorption intensity at 788 cm^{-1} ascribed to the epoxy group was used to calculate the DC for E2.[35,36,61–63]

The kinetic data were converted to $R_p/[M]_0$ by taking the first derivative of the time versus conversion curve,[54,64,65] where and $[M]_0$ are the rate of polymerization and the initial monomer concentration, respectively.

2.4. Preparation of Adhesive Polymer Specimens

The preparation of the polymer specimens has been reported.[65–69] In brief, square beams with a side of 1 mm and a length of at least 15 mm were prepared by injecting the adhesive formulations into glass-tubing molds (Fiber Optic Center, Inc., Part No.: ST8100, New Bedford, MA). Ten specimens were prepared for each formulation. The samples were light polymerized with an light emitting diode (LED) light curing unit for 40 s (LED Curebox, 200 mW cm^{-2} irradiance, Prototech, Portland, OR). It is noted that in our experiments, the polymerization kinetics study is conducted at higher light intensity (550 mW cm^{-2}, halogen light) than the beam specimen preparation conditions (LED curing box, 200 mW cm^{-2}). The beam specimens were prepared using LED light, which has a higher efficiency to induce the photo polymerization. The light sources and the intensity settings have been adjusted so that the degree of conversion and polymerization rate are matched between the systems under these two conditions (unpublished data). The polymerized samples were stored in the dark at room temperature for 48 h to allow for postcure polymerization. It is noted that the degree of conversion at the end of the 48 h storage could be higher than the immediate conversion at 10 min obtained from the reaction kinetics analysis. The samples were extracted from the glass tubing and characterized using dynamic mechanical analysis (DMA) and micro-X-ray computed tomography.

2.5. Characterization

The microscale morphologies of the square beams were observed using 3D micro X-ray computed tomography (MicroXCT-400, Xradia Inc. Pleasanton, CA). Computed tomography facilitates viewing of an object in 3D and allows selection of virtual slices spaced by 1 μm, thus illustrating the bulk structure of heterogeneous materials. As described,[65] the transmission X-ray imaging of the samples was performed using an X-ray tube with a tungsten anode setting of 50 KV at 8 W and an optical magnification of 20×. The 3D images were constructed with the software “XM Reconstructor 8.0” (Xradia Inc. Pleasanton, CA), using 1600 images taken at 12 s exposure time per image.

As reported,[70] the thermal behavior of the adhesive polymers was measured with a TA instruments model Q100 MTDSC (New Castle, DE), equipped with a refrigerated cooling system. The specimens were weighed (15–20 mg) in aluminum DSC pans. The DSC cell was purged with nitrogen gas at 50 mL min^{-1}, and the specimens were heated from −20 to 200 °C at 3 °C min^{-1} with a modulation period of 60 s and an amplitude of ±2 °C.

The viscoelastic properties of the adhesives were characterized using DMA Q800 (TA Instruments, New Castle, USA) with a three-point bending clamp.[65,67,69] The test temperature was varied from 0 to 250 °C with a ramping rate of 3 °C min^{-1}, a frequency of 1 Hz, an amplitude of 15 μm, and a preload of 0.01 N. The properties measured under this oscillating loading were storage modulus (E') and tan δ. The ratio of the loss modulus (E'') to the storage modulus E' is referred to as the mechanical damping, or tan δ (i.e., tan $\delta = E''/E'$). The glass transition temperature (T_g) was determined to be the position of the maximum on the tan δ versus temperature plot. Five specimens of each adhesive formulation were measured under dry conditions, and the results from the five specimens per each formulation were averaged.

2.6. Statistical Analysis

The results were analyzed statistically using analysis of variance, together with Tukey's test at $\alpha = 0.05$ (Microcal Origin Version 8.0, Microcal Software Inc., Northampton, MA).

3. Results and Discussion

3.1. Effect of Coinitiators (Electron Donors) on Cationic Ring-Opening Polymerization of Epoxides

A three-component system for visible light initiation has been widely used in free-radical polymerization. The system generally contains a light absorbing photosensitizer (such as CQ), an elector donor (typically an amine compound), and a third component (often a diaryliodonium or sulfonium salt). The electron donor plays a critical role in the photoinitiation process. A photo-induced electron transfer must take place between the electron acceptor (the photosensitizer) and the electron donor, as seen in Figure 1.[49] Only a few amines are effective in initiating cationic polymerization of epoxides, due to the pivotal role of the electron donor basicity. Protonation of the electron donor may compete with the cationic propagation reaction.[44]

The results of the comparison between DMAEMA and EDMAB when either is used as the coinitiator in a three-component initiator system for E1 cationic ring-opening polymerization are shown in Figure 2. When EDMAB was used as the coinitiator, the DC of the epoxy groups varied from 59.9% (0.5/0.5/1.0 wt%) to 68.0% (2.0/2.0/4.0 wt%), as shown in Table 2. In comparison, there was almost no detectable conversion when DMAEMA was used as the coinitiator. The results demonstrated that the aliphatic amine (DMAEMA) is not suitable as the electron donor in cationic polymerization due to its high basicity; an aliphatic amine can act as the terminator in cationic polymerization. The aromatic amine (EDMAB) has low basicity and was a good coinitiator of cationic ring-opening polymerization. This result was consistent with the previous research on coinitiators.[44] EDMAB was used for further study in this work.

3.2. Effect of Concentration of Initiators on the Kinetics of the Hybrid Polymerization

The results of the polymerization kinetics, of the hybrid system (siloxane epoxy–E1 and methacrylate–HEMA/BisGMA) cured with the three-component initiator system, are shown in Figure 3 and Table 2. Three different weight concentrations (similar range as the commercial products) of CQ/EDMAB/OPPIH (0.5/0.5/1.0, 1.0/1.0/2.0, and 2.0/2.0/4.0 wt%) were studied. The DC for methacrylates and epoxy groups versus the content of siloxane epoxy–E1 are shown in Figure 3A. With the increase of E1 content, the DC of the methacrylates first increased, then decreased when the content of E1 increased over 50 wt% for all of the initiator concentrations. The first increase is attributed to the effect of dilution when introducing E1 into the methacrylate. Similar effects have been observed when water or another solvent was added into methacrylate-based dentin adhesive formulations.[65] The decrease when the content of E1 was over 50 wt% could be attributed to several factors. The mobility of free radicals will be enhanced by the effect of dilution, but the termination effect for polymer radicals could also be enhanced when the concentration of the methacrylates decreases with the increase in E1 concentration (viscosity was decreased). Chain

propagation will be restricted when the concentration of methacrylate monomers is low. In addition, microphase separation between poly(methacrylate) and siloxane-containing polyether (formed from ring-opening polymerization of siloxane-epoxy) in the hybrid system could also have contributed to the decreased DC when the concentration of E1 was over 50 wt%.

With a decrease in the content of E1 (increase of methacrylates), the DC of the epoxy groups decreased when the ratios of CQ/EDMAB/OPPIH were 0.5/0.5/1.0 and 2.0/2.0/4.0 wt%. Mobility restriction of the epoxy monomers as a result of the free radical polymerization could have contributed to the decreased DC. The lowest DC of the epoxy groups was obtained when the ratio of CQ/EDMAB/OPPIH was 0.5/0.5/1.0 wt%. There was no significant difference in the DC of the epoxy groups at the ratio of 1.0/1.0/2.0 wt% with decreasing E1 content. It should be noted that the lowest content of the E1 monomer for the kinetics study of the epoxy groups was 50 wt%. The FTIR spectra of the epoxy groups overlapped substantially with the absorbance peaks of different C–H bonds of the methacrylates if the epoxy content was lower than 50 wt%.

The polymerization rates for the methacrylates and the ring-opening rates of the epoxy groups versus the content of E1 are shown in Figure 3B and Table 2. With increasing E1 content, the polymerization rate ($R_p/[M]_0$) of the double bonds decreased because of the reduced methacrylate concentration. Moreover, at the same E1 content, the $R_p/[M]_0$ of free radical polymerization was similar to that in the presence of different concentrations of initiators (Table 2). These $R_p/[M]_0$ values are the result of the auto-acceleration effect in free radical polymerization, which is associated with the viscosity of the monomer resin.

For the ring-opening rate of the epoxy monomer (it should be noted, the ring-opening rate includes the polymerization rate and chain transfer rate of reaction between epoxy and hydroxyl groups in methacrylates), decreasing behavior was also observed with increasing content of the methacrylates (decreasing the content of E1). The ring-opening rate of the epoxy groups was much lower than that of the free radical polymerization (Figure 3B). The rate associated with the epoxy groups is likely influenced by the exothermic reaction and increased viscosity associated with the free radical polymerization of the methacrylates. This may account for the narrowing of the rate difference between the epoxy groups with increasing methacrylate content at different initiator concentrations; the $R_p/[M]_0$ of free radical polymerization is similar at different initiator concentrations. Considering the DC of the epoxy groups, the weight percentage for the initiators of (CQ/EDMAB/OPPIH = 1.0/1.0/2.0 wt%) was used for further research.

3.3. Comparison of the Kinetics Between E1 (Siloxane Epoxy) and E2 (Oxocarbon Epoxy) in Free-Radical/Cationic Ring-Opening Hybrid Polymerization

IPNs are formed when two distinct functional polymers become entangled at the molecular level. In general, phase separation will happen if the miscibility of the polymers is low. Polymerization kinetics also plays an important role in the final structure and properties of the IPN. To understand the effect of chemical miscibility and the individual kinetics of each polymerization mechanism on the final structures and properties of the IPN, two types of epoxy monomers were used in this study. E1 is a siloxane-containing epoxy monomer,

which was reported with higher reactivity[53] and a similar structure to that used in silorane composite (Filtek LS by 3M/ESPE, St. Paul, MN). E2 is a commercial oxocarbon epoxy monomer, which was widely used in industry.[35,36,63]

The results of the kinetics comparison for epoxy monomers (E1 vs E2) in the hybrid polymerization system are shown in Figure 4. As noted in Figure 4A, the DC of the E1-containing system (65%–68%) was much higher than that of the E2-containing system (36%–40%). This difference could be due to the higher reactivity of the siloxane epoxy monomer. As shown in Figure 4B and Table 2, the reaction rate of pure E1 (without methacrylates) (0.11 s^{-1}) was more than twice the rate of pure E2 (0.05 s^{-1}). With the increase of methacrylate content in the hybrid system, the ring-opening rate for both E1 and E2 decreased due to the decrease in epoxy concentration. Another reason for this rate decrease was noted by Crivello and colleagues, i.e., the presence of ester groups greatly retards the ring-opening rate of epoxy groups because of the nucleophilic property of the ester group.[71] Furthermore, the ring-opening rate for E1 was always higher than that of E2 with the same content of methacrylates (as shown in Figure 4B and Table 2) due to the higher activity of siloxane-epoxy.[53]

Methacrylate polymerization kinetics in the presence of different epoxy monomers is shown in Figure 5. As seen from Figure 5A,B, the DC of the methacrylates increased initially with increasing epoxy content for both E1 and E2. The DC of methacrylates decreased when the E1 content was above 50 wt%. In comparison, for the E2-containing system, although there was a slight decrease in DC when the E2 content was above 50 wt%, the DC was significantly higher than the control. This may be attributed to the poor miscibility between siloxane-containing polyether and poly(methacrylate).[72–78] The results of the $R_p/[M]_0$ for methacrylate groups are shown in Figure 5C,D. With increasing epoxy content, the $R_p/[M]_0$ decreased due to the reduced methacrylate concentration. In addition, the greater mobility restriction imposed by the cationic polymerization process might be the second reason for the decreased R_p of methacrylates. As seen from Figure 5E, at the same epoxy content, the $R_p/[M]_0$ of methacrylate with E2 was slightly higher than that with E1. This may be attributed, in part, to differences in the viscosities of the epoxy monomers, i.e., pure E1 (140.0 cP) had a lower viscosity than pure E2 (381.0 cP) (Supporting Information). The maximum R_p in our study was associated with the autoacceleration effect of polymerization. With lower viscosity, the autoacceleration effect would be depressed compared with higher viscosity system. Thus, a lower epoxy viscosity translates to a lower maximum R_p (More explanation about the relationship between polymerization rate and auto acceleration effect is provided in the Supporting Information).

3.4. Microphase Separation and Acceleration Effect of Cationic Ring-Opening Reaction

The Micro CT images of E1-50 and E2-50 formulations are shown in Figure 6. Distinct contrast is noted in the Micro CT images if there are different phases in the materials. The concentric rings at the top of the cylinder are noted in all of the images and these rings are associated with individual pixel response.[79,80] Microphase separation is observed in the E1-50 formulations (Figure 6A). In contrast, no microphase separation was detected when 50 wt% E2 was used. Several factors may explain these results. There could be limited

miscibility between siloxane-containing polyether and poly(methacrylate) and thus, microphase separation happened during formation of the IPN.[72–78] The difference in the polymerization rate for the methacrylate double bond and the ring-opening rate for the epoxy mono mer could contribute to microphase separation. During the free-radical/cationic hybrid polymerization process, the polymerization rate of free radical polymerization is much higher than that of the cationic ring-opening reaction (Figure 3 and Table 2). As seen from Figure 7, with 50 wt% epoxy monomer, the $R_p/[M]_0$ of methacrylate was much higher than the ring-opening rate of the epoxy groups for both E1 and E2-containing formulations. This result supports microphase separation in the E1-50 formulation because of poor miscibility between siloxane-containing polyether and poly(methacrylate).[72–78]

Phase separation could lead to undesirable properties in the final polymer and thus, it is important to find a way to depress the phase separation. As reported by Crivello and colleagues, acetal and vinyl ether groups can be used as accelerators for cationic polymerization.[25,81] Therefore, GBDA was used in this study, for the first time, to accelerate the cationic ring-opening polymerization and to determine if modulation of the polymerization kinetics could influence the microphase separation.

As seen from Table 2, after acceleration of the cationic ring-opening reaction, the maximum ring-opening rate ($R_p/[M]_0$) of the epoxy groups increased from 0.02 s^{-1} (E1-50) to 0.06 s^{-1} (E1-50-10). In contrast, the maximum free radical polymerization rate decreased from 0.12 s^{-1} (E1-50) to 0.08 s^{-1} (E1-50-10) because 10 wt% of the methacrylate concentration was replaced by accelerator-GBDA. The maximum ring-opening rate (0.06 s^{-1}) was only slightly lower than that of the methacrylates (0.08 s^{-1}) in the hybrid system, as shown in Figure 8A (In addition, there was a second maximum peak, which might be attributed to the micro gel formation.[82] Some pendant double bonds became trapped within the microgel, limiting their availability. These species become reactive at some point during the reaction, leading to a secondary maximum or triggering a second Trommsdorff effect). No microphase separation is noted in the representative image of polymer specimens cured in the presence of accelerator (Figure 8B). This result indicates that microphase separation can be depressed by manipulating the reaction rate for both the methacrylate and epoxy monomers.

When rates for both polymerization processes are similar, sufficient crosslinking of the components in the IPN may occur at a similar pace before diffusion of the components occurs. Thus, interlocking of the two networks within the IPN prevents microphase separation.[83–85] There may be, however, phase separation at the nano-scale because of a lack of chemical miscibility. Indeed, the polymer beams cured in the presence of the accelerator were not as transparent as those made from the control formulation, although the morphology of the whole beam appeared homogeneous. To our knowledge, this is the first time that microphase separation in the hybrid polymerization system has been modulated by introducing an accelerator for the cationic polymerization.

Generally, polymers with siloxane groups are usually soft, and their mechanical strength is low because of the flexibility of the siloxane groups.[86,87] A lower content of siloxane-containing monomers is desirable for applications such as dentin adhesives. The hybrid system with and without accelerator was studied at 25 wt% E1. Without accelerator, there

was no microphase separation (Figure 9A), while microphase separation is clearly visible in the samples made in the presence of accelerator (E1-25-10, Figure 9B). These results are in distinct contrast to the results with the E-50 formulations. To explain these differences, we propose a mechanism of microphase separation in the free-radical/cationic ring-opening polymerization (Figure 10).

For the formulations of E1-50 (Figure 10A), the R_p of epoxy monomer (it should be noted that the R_p is the ring-opening rate for the epoxy monomer) was accelerated to a value similar to that of methacrylate in the formulation of E1-50-10 (Figure 10B). This similarity in R_p depressed the phase separation in the polymer beam. As shown in Figure 10C, the R_p of epoxy for E1-25 should be lower than that of E1-50 due to the lower E1 concentration. After acceleration of the cationic ring-opening reaction (E1-25-10), the R_p of epoxy was very likely similar to that of E1-50, but still lower than that of the methacrylates. This may account for similar results in terms of microphase separation for the formulations E1-50 and E1-25-10. These results indicate that when the siloxane epoxy content is lower than 25 wt%, the accelerator for cationic polymerization will cause microphase separation. In contrast, at high siloxane epoxy content (higher than 50 wt%), the accelerator will prevent microphase separation.

There was no microphase separation detected with low E1 content (≤25 wt%), e.g., E1-5, E1-15 and E1-25. At these concentrations, the polymer beams were as transparent as the control formulations. A possible explanation is that the epoxy groups of E1 can undergo chain transfer reaction with the hydroxyl groups of the methacrylates (Figure 10E). That is, there might not be a separated siloxane-containing phase (or the chain length of siloxane-containing polyether is very short). In other words, E1 may act as the crosslinker to enhance the crosslinking density of the poly(methacrylate) network, and the chain transfer reaction may act as the compatibilizer to prevent microphase separation between siloxane-containing polyether and poly(methacrylate).[63] This type of chain transfer reaction has been reported by other investigators.[88,89] For example, the chain transfer reaction between the epoxy groups and the hydroxyl groups of HEMA can be used to develop a new type of crosslinking technology for coating systems,[88] and can also be used in dental composites.[89] In recent work by Jessop et al.,[63] the chain transfer effect was investigated for the epoxy monomer under cationic photopolymerization, and their results show the chain transfer effect can be used to tune the crosslinking densities of epoxy resins. These results indicate that in the hydroxyl-containing system, the chain transfer effect is significant. In our system, both HEMA and BisGMA contain hydroxyl groups and thus, a chain transfer reaction with epoxy was expected. This is the first time that the free-radical/cationic ring-opening hybrid polymerization initiated by visible light has been studied in relationship to the chain transfer effect between epoxy and hydroxyl groups of methacrylates. The results are valuable in the design and development of new durable coating/adhesive systems.

3.5. Crosslinking Structure Study by Modulated DSC

When designing a cross-linked polymer for a specific application, it is important to understand the structure of the network. Modulated DSC, in which a small temperature modulation is applied to the underlying linear temperature program, has been used to study

photo-initiated acrylate-based polymer resin.[70] The results of the reversible heat flow, nonreversible heat flow, and derivative reversible heat flow for the control and E1-25 are shown in Figure 11A,B. The glass transition temperature, which is a reversible phenomenon, is clearly observed on the derivative reversible heat flow curves. The curves for C0 and E1-25 both show a lower transition temperature at about 60 °C and a higher transition temperature above 100 °C. The higher transition temperature decreased from 130 °C (C0) to 102 °C (E1-25), which was attributed to the incorporation of the flexible siloxane groups. Both of the transition peaks at about 60 °C were attributed to the lower crosslinking region in the network.[70] This result suggests that there was negligible or no separated siloxane-containing phase in the E1-25 formulation. The chain transfer reaction between epoxy and hydroxyl groups could be a reasonable explanation for this observation.

E1-25-10 showed a broad transition peak at low temperature in the presence of accelerator (Figure 11C). This is caused by the microphase separation between the siloxane-containing polyether and poly(methacrylate) as a result of the acceleration of the cationic ring-opening polymerization (E1-25-10). After acceleration, the chain of siloxane-containing polymer could grow longer than the formulation without the accelerator. When the chain length of siloxane-containing polymer grows to a certain length, phase separation with poly(methacrylate) may occur.[83] This result could be correlated with the microphase separation noted in the Micro CT images.

The modulated DSC results further support that the majority of the epoxy monomer may act as the crosslinker in the formulation of E1-25, and there was no separation of the siloxane-containing phase from the poly(methacrylate) phase. The curve of E1-50 shows a similar shape to the curve of E1-25-10 (Figure 11C). After acceleration, the ring-opening rate of epoxy in E1-25-10 might be similar to E1-50 (higher epoxy concentration). The curve of E1-50-10 (Figure 11C) shows that the transition temperature further decreased because the siloxane-containing part was enhanced by the acceleration of cationic ring-opening polymerization.

3.6. DMA Under Dry Conditions

Polymers with siloxane groups are usually soft because of the flexibility of Si–O bonds.[86,87] Therefore, from an application point of view, enhancement of the mechanical properties is important for siloxane-containing polymers. To delineate the relationship between the mechanical property, chemical structure, and weight content of the epoxy monomers in systems cured by free radial/cationic ring-opening hybrid polymerization, polymer resins with 5, 15, and 25 wt% epoxy monomer (E1 and E2) with methacrylate were characterized. (It should be noted that, when the epoxy content is higher than 25 wt%, the polymerized beams are very brittle.)

Because DMA gives information about the relaxation of molecular motions, which are sensitive to structure and variation in the stiffness of materials, it can be used to provide information on the properties of polymer networks, such as storage modulus and glass transition temperature.[67,69] The results of DMA under dry conditions for the control and experimental polymers are shown in Figure 12. Figure 12A,B show the storage modulus (E') as a function of temperature for the hybrid system cured in the presence of E1 and E2,

respectively. The storage modulus values for all of the samples decreased with an increase in temperature. Figure 12C,D show the derivative storage modulus versus temperature curves. There were two transition peaks for each formulation. For example, the curve for C0 showed a lower transition temperature at about 80 °C and a higher transition temperature at about 128 °C. With an increase in the epoxy content (Figure 12C,D), the peak intensity at the lower transition temperature becomes very clear and the peak intensity at the higher transition temperature is decreased. The increase of peak intensity at the lower temperature is attributed to the chain transfer reaction between epoxy and hydroxyl groups of methacrylate. As reported, the lower temperature transition peak corresponds to the ß-transition of the side-chains of the methacrylates.[90] The results, presented in Figure 12C,D, indicate that the side-chains are different from the control. This difference is attributed to the chain transfer reaction between the epoxy and hydroxyl groups of the methacrylates, as discussed previously. Moreover, these DMA results were consistent with those from modulated DSC and Micro CT, and further support the hypothesis in Figure 10.

The results of the tan δ versus temperature curves for E1 and E2-containing polymers with different weight content are shown in Figure 12E,F. The intensity of the maximum tan δ peak reflects the mobility of the polymer chain segments at this temperature. For E1, the intensity of the maximum tan δ peak decreased from 0.74 (C0) to 0.57 (E1-25). In comparison, the intensity of the maximum tan δ peak decreased from 0.74 (C0) to 0.65 (E2-25) with E2. These results indicate less mobility of the polymer chains with the incorporation of E1 as compared to E2. At the same time, the T_g decreased from 147.3 °C (C0) to 139.8 °C (E1-25) and 127.9 °C (E2-25). Full-width-at-half-maximum (FWHM) of the tan δ peaks for the experimental formulations were greater than those of the control (Table 3); these results indicate that the glass transition occurs over a wide temperature range. This broad glass transition can be attributed to heterogeneous networks containing regions with different crosslinked structure (highly crosslinked and less densely crosslinked regions), resulting in broad distribution of mobilities or relaxation times.[67,91] Generally, the wider tan δ peaks (higher heterogeneous networks) usually appear with an increase in the crosslink density of the polymer networks.[67–69] The wide tan δ peaks support higher crosslinking density caused by the chain transfer reaction between epoxy and hydroxyl groups.

As shown in Figure 12G, the values of the storage modulus at 37 °C were similar to the control, although there was a slight decrease for the storage modulus values when E1 (siloxane epoxy) content was increased to 25 wt%. For E2-containing polymers, the storage modulus at 37 °C was similar to the control. The results of the storage modulus at 180 °C are shown in Figure 12H. The values for E1-containing polymers at 180 °C at the rubbery region[67,68] were similar to the control formulation (C0). The values for E2-containing polymers were slightly higher than the control, as shown in Figure 12H and Table 3. This difference could be attributed to the flexibility of the siloxane groups. Although the entanglement of polymer chains was enhanced by the chain transfer reaction of epoxy with hydroxyl groups (decreased tan δ intensity, as shown in Figure 12E), the apparent value of the storage modulus at the rubbery region appears similar to the control for E1-containing adhesives. Without the chain transfer reaction, the values of the storage modulus at 180 °C would be lower than the control formulation (C0) due to the incorporation of flexible

siloxane components. It should be noted that the values of the storage modulus at 180 °C for E2-containing adhesives, shown in Figure 12H, were affected by the postring-opening reaction of the E2 mono mer. Because of the lower DC of E2, under higher temperatures, the residual E2 monomer will ring-open and crosslink with the hydroxyl groups of the methacrylates by the chain transfer reaction.

The network formed by the hybrid system should be further crosslinked by the chain transfer reaction between the epoxy and hydroxyl groups of methacrylate. In order to further investigate the crosslinking structure and mechanical properties, DMA experiments of specimens cured in the presence/absence of accelerators were conducted. The presence of an accelerator (GBDA) of a cationic ring-opening reaction led to a decrease in storage modulus of the E1-25 formulations (E1-25-10 vs E1-25, Figure 13A and Table 3). This may be attributed to phase separation of the siloxane-containing polymer as a result of the accelerator (such phase separation is noted in results from the modulated DSC (Figure 11) and Micro CT (Figure 9). An additional explanation is that siloxane-containing polyether is softer than poly(methacrylate). This result further supports the chain transfer reaction in the absence of acceleration of the cationic polymerization. Otherwise, the storage modulus of the specimens should be much lower than the control. As shown in Figure 13B, the intensity of the tan δ peak for E1-25-10 (after acceleration), 0.46 in Table 2, was much lower than E1-25, 0.57 in Table 2. The decreased intensity of the tan δ peak might be attributable to higher crosslinking density as a result of the chain transfer reaction. Although cationic ring-opening polymerization can be enhanced by the presence of an accelerator, the chain transfer reaction between epoxy and hydroxyl groups could also be enhanced. In addition, as seen from Figure 13B, there was a new peak in the tan δ curve at 30.8 °C, which could be attributed to the siloxane-containing phase. This DMA result coincides with the result obtained from modulated DSC and Micro CT, and further supports the proposed mechanism in Figure 10.

This fundamental study of hybrid radical/cationic photopolymerization is the first step towards our design and development of versatile dentin adhesives. With wet bonding techniques, the channels between the demineralized dentin collagen fibrils are filled with water, solvent, conditioner, and/or oral fluids. It is noted that in this investigation we focused on neat resin instead of water-containing systems. The study of the effect of water on the cationic and free radical polymerization in the hybrid system is important for applications involving dentin bonding agents. This work is ongoing.

4. Conclusion

Polymerization kinetics of free-radical/cationic ring-opening hybrid polymerization under visible light was studied in detail by employing varying concentrations of three-component initiators and different monomer contents. The kinetics results show that the epoxy ring-opening rate is much lower than the rate of free radical polymerization. In addition to the effect of polymerization kinetics, the effect of chemical miscibility on the crosslinking structure was also studied by using different epoxy monomers: siloxane epoxy and oxocarbon epoxy. The acceleration effect for cationic ring-opening polymerization was investigated and these results indicate that when the siloxane epoxy content is lower than 25

wt%, the presence of accelerator will cause microphase separation. For formulations with high siloxane epoxy content, i.e., ≥50 wt%, the presence of accelerator for cationic polymerization will prevent microphase separation. The results from these investigations support the chain transfer reaction between epoxy and hydroxyl groups of the methacrylate. The experimental results suggest that the chain transfer reaction enhances the crosslinking density and prevents micrometer-level phase separation. The chain transfer reaction was further investigated using modulated DSC and DMA. The DMA results show that the mechanical properties of polymers formed by visible-light initiated free-radical/cationic ring-opening hybrid polymerization were comparable to the control adhesive formed by free radical polymerization. These results provide important structure/property relationships for hybrid polymerization and information that may be useful for future development of durable, versatile coatings/adhesives.

Supplementary Material

Refer to Web version on PubMed Central for supplementary material.

Acknowledgments

This investigation was supported by Research Grant: R01 DE022054 and R01 DE022054-04S1 from the National Institute of Dental and Craniofacial Research, National Institutes of Health, Bethesda, MD.

References

1. Sperling LH. Macromol Rev. 1977; 12:141.
2. Sperling LH. Adv Chem Ser. 1986:21.
3. Baidak AA, Liegeois JM, Sperling LH. J Polym Sci, Part B: Polym Phys. 1997; 35:1973.
4. Degirmenci M, Hepuzer Y, Yagci Y. J Appl Polym Sci. 2002; 85:2389.
5. Guo HQ, Kajiwara A, Morishima Y, Kamachi M. Macromolecules. 1996; 29:2354.
6. Hawker CJ, Hedrick JL, Malmstrom EE, Trollsas M, Mecerreyes D, Moineau G, Dubois P, Jerome R. Macromolecules. 1998; 31:213.
7. Mecerreyes D, Moineau G, Dubois P, Jerome R, Hedrick JL, Hawker CJ, Malmstrom EE, Trollsas M. Angew Chem Int Ed. 1998; 37:1274.
8. Mecerreyes D, Atthoff B, Boduch KA, Trollsas M, Hedrick JL. Macromolecules. 1999; 32:5175.
9. Mecerreyes D, Pomposo JA, Bengoetxea M, Grande H. Macromolecules. 2000; 33:5846.
10. Braun H, Yagci Y, Nuyken O. Eur Polym J. 2002; 38:151.
11. Kan CY, Liu DS, Kong XZ, Zhu XL. J Appl Polym Sci. 2001; 82:3194.
12. Mecerreyes D, Humes J, Miller RD, Hedrick JL, Detrembleur C, Lecomte P, Jerome R, San Roman J. Macromol Rapid Commun. 2000; 21:779.
13. Decker C, Viet TNT, Decker D, Weber-Koehl E. Polymer. 2001; 42:5531.
14. Suthar B, Xiao HX, Klempner D, Frisch KC. Polym Adv Technol. 1996; 7:221.
15. Dowbenko R, Friedlander C, Gruber G, Prucnal P, Wismer M. Prog Org Coat. 1983; 11:71.
16. Rose K, Vangeneugden D, Paulussen S, Posset U. Surf Coat Int, Part B. 2006; 89:41.
17. Schroeter SH. Annu Rev Mater Sci. 1975; 5:115.
18. Senich GA, Florin RE. J Macromol Sci, Rev Macromol Chem. 1984; C24:239.
19. Spencer P, Wang Y. J Biomed Mater Res. 2002; 62:447. [PubMed: 12209931]
20. Cho JD, Hong JW. J Appl Polym Sci. 2004; 93:1473.
21. Cook WD, Chen F, Ooi SK, Moorhoff C, Knott R. Polym Int. 2006; 55:1027.
22. Dean K, Cook WD, Zipper MD, Burchill P. Polymer. 2001; 42:1345.

23. Dean KM, Cook WD. Polym Int. 2004; 53:1305.
24. Decker C, Zahouily K, Decker D, Nguyen T, Viet T. Polymer. 2001; 42:7551.
25. Rajaraman SK, Mowers WA, Crivello JV. J Polym Sci, Polym Chem Ed. 1999; 37:4007.
26. Rajaraman SK, Mowers WA, Crivello JV. Macromolecules. 1999; 32:36.
27. Decker C, Bianchi C, Decker D, Morel F. Prog Org Coat. 2001; 42:253.
28. Sangermano M, Malucelli G, Morel F, Decker C, Priola A. Eur Polym J. 1999; 35:639.
29. Chaplelow CC, Pinzino CS, Chen SS, Jeang L, Eick JD. J Appl Polym Sci. 2007; 103:336.
30. Cramer NB, Stansbury JW, Bowman CN. J Dent Res. 2011; 90:402. [PubMed: 20924063]
31. Weinmann W, Thalacker C, Guggenberger R. Dent Mater. 2005; 21:68. [PubMed: 15681004]
32. Lin Y, Stansbury JW. Polymer. 2003; 44:4781.
33. Lecamp L, Pavillon C, Lebaudy P, Bunel C. Eur Polym J. 2005; 41:169.
34. Ortiz RA, Sangermano M, Bongiovanni R, Valdez AEG, Duarte LB, Saucedo IP, Priola A. Prog Org Coat. 2006; 57:159.
35. Cai Y, Jessop JLP. Polymer. 2006; 47:6560.
36. Cai Y, Jessop JLP. Polymer. 2009; 50:5406.
37. Chen F, Cook WD. Eur Polym J. 2008; 44:1796.
38. Nowers JR, Narasimhan B. Polymer. 2006; 47:1108.
39. Jakubiak J, Allonas X, Fouassier JP, Sionkowska A, Andrzejewska E, Linden LA, Rabek JF. Polymer. 2003; 44:5219.
40. Kim D, Stansbury JW. J Polym Sci, Part A: Polym Chem. 2009; 47:887.
41. Crivello JV. J Polym Sci, Part A: Polym Chem. 2009; 47:866.
42. Crivello JV, Ortiz RA. J Polym Sci, Part A: Polym Chem. 2002; 40:2298.
43. Crivello JV, Sangermano M. J Polym Sci, Part A: Polym Chem. 2001; 39:343.
44. Bi YB, Neckers DC. Macromolecules. 1994; 27:3683.
45. Lalevee J, Dirani A, El-Roz M, Allonas X, Fouassier JP. J Polym Sci, Part A: Polym Chem. 2008; 46:3042.
46. Lalevee J, Dirani A, El-Roz M, Allonas X, Fouassier JP. Macromolecules. 2008; 41:2003.
47. Lalevee J, El-Roz M, Allonas X, Fouassier JP. J Polym Sci, Part A: Polym Chem. 2008; 46:2008.
48. Lalevee J, Tehfe MA, Morlet-Savary F, Graff B, Allonas X, Fouassier JP. Prog Org Coat. 2011; 70:23.
49. Oxman JD, Jacobs DW, Trom MC, Sipani V, Ficek B, Scranton AB. J Polym Sci, Part A: Polym Chem. 2005; 43:1747.
50. Flory PJ. J Chem Phys. 1941; 9:660.
51. Huggins ML. J Chem Phys. 1941; 9:440.
52. Crivello JV, Lee JL. ACS Symp Ser. 1990; 417:398.
53. Crivello JV, Lee JL. J Polym Sci, Part A: Polym Chem. 1990; 28:479.
54. Jang M, Crivello JV. J Polym Sci, Part A: Polym Chem. 2003; 41:3056.
55. Ye Q, Park JG, Topp E, Wang Y, Misra A, Spencer P. J Dent Res. 2008; 87:829. [PubMed: 18719208]
56. Park J, Ye Q, Topp EM, Misra A, Kieweg SL, Spencer P. J Biomed Mater Res A. 2010; 93A:1245.
57. Ye Q, Park J, Topp E, Spencer P. Dent Mater. 2009; 25:452. [PubMed: 19027937]
58. Song LY, Ye Q, Ge XP, Misra A, Laurence JS, Berry CL, Spencer P. J Biomed Mater Res B. 2014; 102:1473.
59. Ge XP, Ye Q, Song LY, Misra A, Spencer P. Dent Mater. 2014; 30:1073. [PubMed: 24993811]
60. Ye QA, Wang Y, Williams K, Spencer P. J Biomed Mater Res B. 2007; 80B:440.
61. Chen Y, Li GL, Zhang HQ, Wang T. J Polym Res. 2011; 18:1425.
62. Kim JY, Patil PS, Seo BJ, Kim TS, Kim J, Kim TH. J Appl Polym Sci. 2008; 108:858.
63. Dillman B, Jessop JLP. J Polym Sci Part A: Polym Chem. 2013; 51:2058.
64. Guo X, Wang Y, Spencer P, Ye Q, Yao X. Dent Mater. 2008; 24:824. [PubMed: 18045679]
65. Park J, Ye Q, Singh V, Kieweg SL, Misra A, Spencer P. J Biomed Mater Res B. 2012; 100B:569.

66. Park J, Eslick J, Ye Q, Misra A, Spencer P. Dent Mater. 2011; 27:1086. [PubMed: 21816460]
67. Park JG, Ye Q, Topp EM, Lee CH, Kostoryz EL, Misra A, Spencer P. J Biomed Mater Res B. 2009; 91B:61.
68. Park JG, Ye Q, Topp EM, Misra A, Spencer P. Dent Mater. 2009; 25:1569. [PubMed: 19709724]
69. Parthasarathy R, Misra A, Park J, Ye Q, Spencer P. J Mater Sci: Mater Med. 2012; 23:1157. [PubMed: 22430592]
70. Ye Q, Spencer P, Wang Y, Misra A. J Biomed Mater Res A. 2007; 80A:342.
71. Crivello JV, Varlemann U. J Polym Sci, Polym Chem Ed. 1995; 33:2473.
72. Abbasi F, Mirzadeh H, Katbab AA. Polym Int. 2001; 50:1279.
73. Frisch HL, Gebreyes K, Frisch KC. J Polym Sci, Polym Chem Ed. 1988; 26:2589.
74. Mera AE, Goodwin M, Pike JK, Wynne KJ. Polymer. 1999; 40:419.
75. Nicolson PC, Vogt J. Biomaterials. 2001; 22:3273. [PubMed: 11700799]
76. Olabisi O. J Chem Educ. 1981; 58:944.
77. Smith SD, DeSimone JM, Huang H, York G, Dwight DW, Wilkes GL, McGrath JE. Macromolecules. 1992; 25:2575.
78. Zhou PG, Frisch HL, Rogovina L, Makarova L, Zhdanov A, Sergeienko N. J Polym Sci, Polym Chem Ed. 1993; 31:2481.
79. Kyriakou Y, Prell D, Kalender WA. Phys Med Biol. 2009; 54:N385. [PubMed: 19661571]
80. Sijbers J, Postnovz A. Phys Med Biol. 2004; 49:N247. [PubMed: 15357205]
81. Crivello JV, Ortiz RA. J Polym Sci, Polym Chem Ed. 2001; 39:2385.
82. Abedin F, Ye Q, Good HJ, Parthasarathy R, Spencer P. Acta Biomater. 2014; 10:3038. [PubMed: 24631658]
83. Lipatov YS, Alekseeva TT. Adv Polym Sci. 2007; 208:1.
84. Lastumaki TM, Lassila LVJ, Vallittu PK. J Mater Sci: Mater Med. 2003; 14:803. [PubMed: 15348401]
85. Vazquez A, Rojas AJ, Adabbo HE, Borrajo J, Williams RJJ. Polymer. 1987; 28:1156.
86. Mark JE. Acc Chem Res. 2004; 37:946. [PubMed: 15609986]
87. Lotters JC, Olthuis W, Veltink PH, Bergveld P. J Micromech Microeng. 1997; 7:145.
88. Wu S, Soucek MD. Polymer. 2000; 41:2017.
89. Tilbrook DA, Clarke RL, Howle NE, Braden M. Biomaterials. 2000; 21:1743. [PubMed: 10905456]
90. Dionysopoulos P, Watts DC. J Dent. 1989; 17:140. [PubMed: 2768624]
91. Singh V, Misra A, Marangos O, Park J, Ye QA, Kieweg SL, Spencer P. J Biomed Mater Res B. 2010; 95B:283.

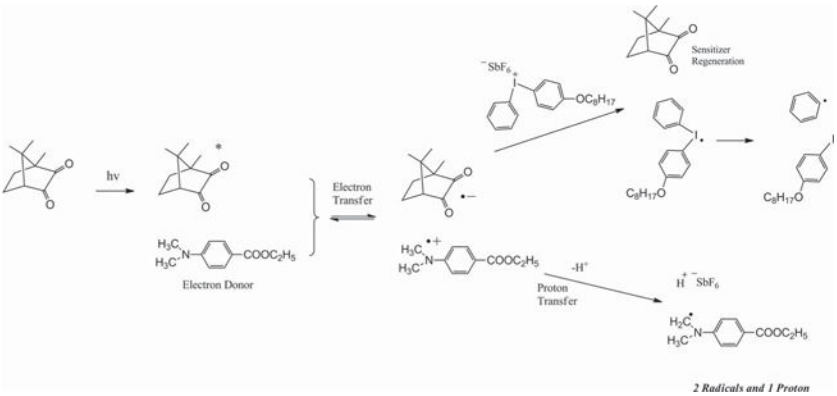

Figure 1.
Initiation mechanism of the three-component initiator system (adapted from[49]).

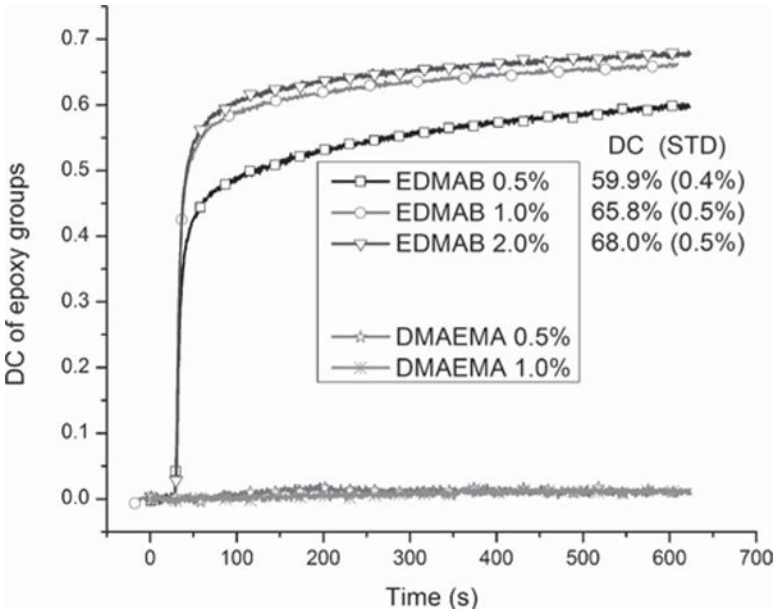

Figure 2.

Real-time conversion of E1 (pure siloxane epoxy) with different amines used as the electron donors (EDMAB and DMAEMA). A three-component initiator system was used: CQ/EDMAB (or DMAEMA)/OPPIH = 1/1/2 (wt). The adhesives were light-cured for 40 s at room temperature using a commercial visible-light-curing unit (Spectrum 800, Dentsply, Milford, DE. Intensity was 550 mW cm^{-2}). Real-time IR spectra were continuously recorded for 600 s after light activation began.

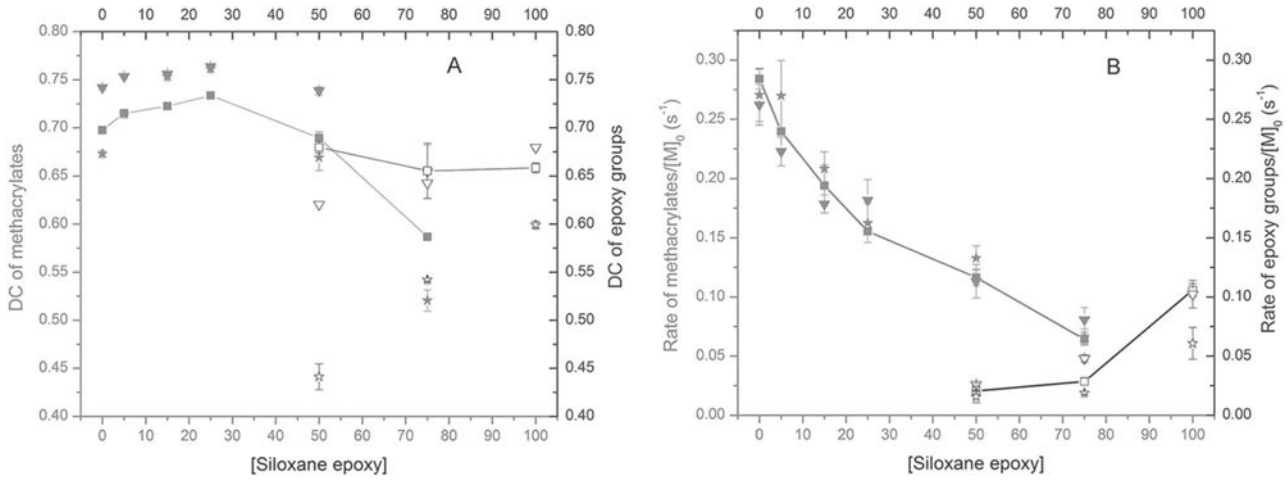

Figure 3.

Degree of conversion for methacrylates and epoxy groups versus the content of E1. A) Polymerization rate for methacrylates and ring-opening rate for epoxy groups versus content of E1. B) A three-component initiator system contains CQ, EDMAB and OPPIH. ★ (methacrylates) and ✯(epoxy groups): CQ/EDMAB/OPPIH = 0.5/0.5/1.0 (wt %); ■ (methacrylates) and □(epoxy groups): CQ/EDMAB/OPPIH = 1.0/1.0/2.0 (wt %); ▼ (methacrylates) and ▽(epoxy groups): CQ/EDMAB/OPPIH = 2.0/2.0/4.0 (wt %).

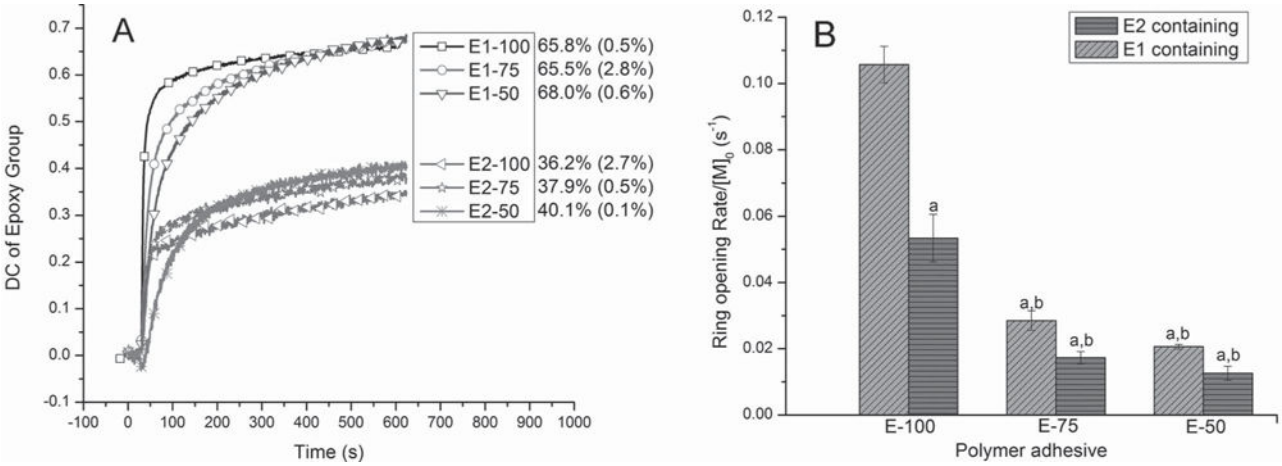

Figure 4.

A) Real-time conversion of epoxy groups for E1 and E2-containing adhesive resins. A three-component initiator system was used: CQ/EDMAB/OPPIH = 1.0/1.0/2.0 (wt%). The adhesives were light-cured for 40 s at room temperature using a commercial visible-light-curing unit (Spectrum 800, Dentsply, Milford, DE. Intensity was 550 mW cm^{-2}). Real-time IR spectra were continuously recorded for 600 s after light activation began. B) The comparison of maximum polymerization rate for E1 and E2-containing adhesive resins. a) Significant ($p < 0.05$) difference from E1-100. b) Significant ($p < 0.05$) difference from E2-100. E-*x*: *x* is the weight content of the epoxy monomers.

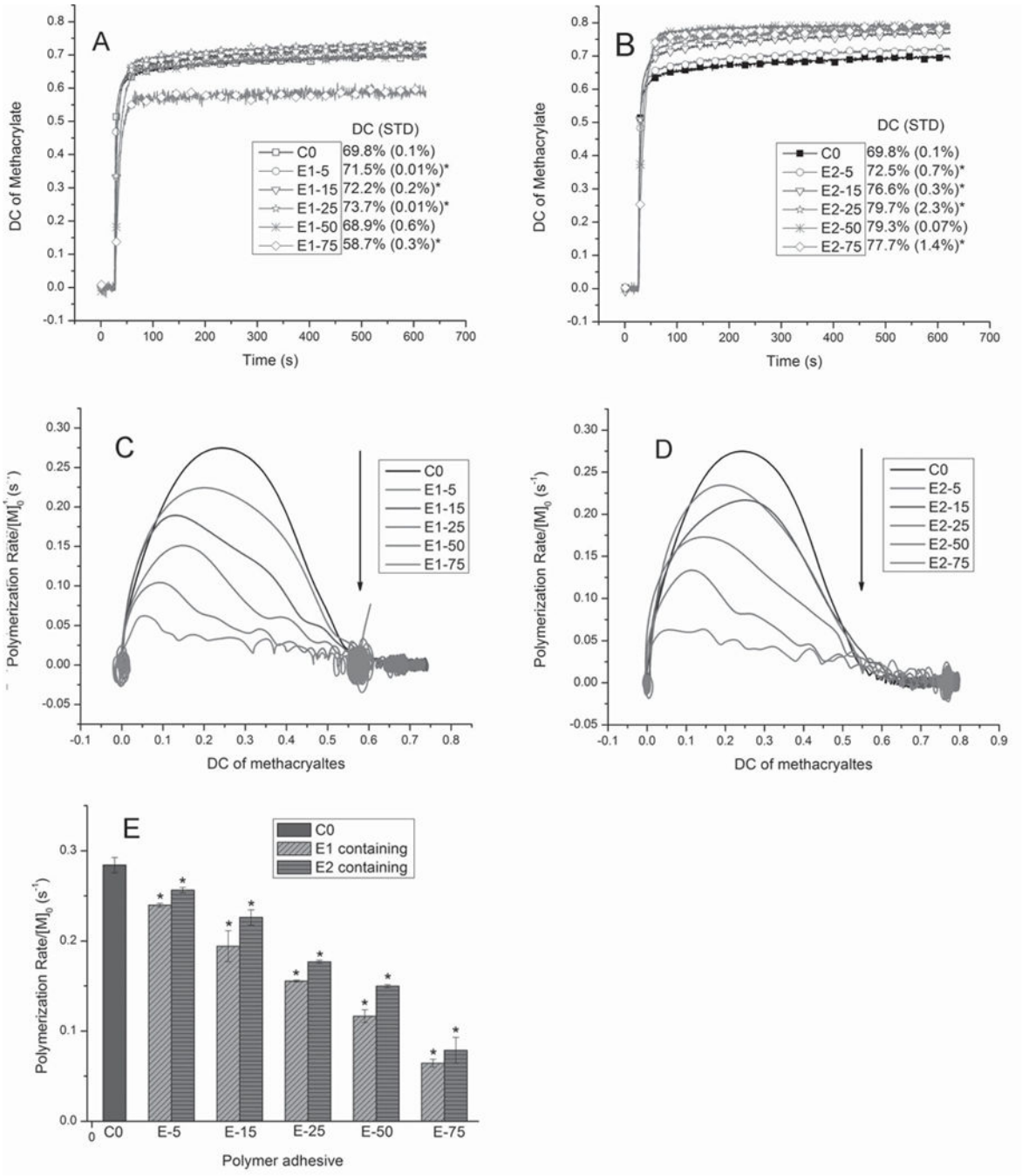

Figure 5.

Real-time conversion of methacrylates for A) E1- and B) E2-containing adhesive resins. A three-component initiator system was used: CQ/EDMAB/OPPIH = 1.0/1.0/2.0 (wt%). The adhesives were light-cured for 40 s at room temperature using a commercial visible-light-curing unit (Spectrum 800, Dentsply, Milford, DE. Intensity was 550 mW cm^{-2}). Real-time IR spectra were continuously recorded for 600 s after light activation began. Polymerization rate of methacrylates versus the DC of methacrylates for C) E1- and D) E2-containing adhesive resins. E) The comparison of maximum polymerization rate for E1- and E2-

containing adhesive resins. *indicates Significant ($p < 0.05$) difference from C0. E-*x*: *x* is the weight content of the epoxy monomers.

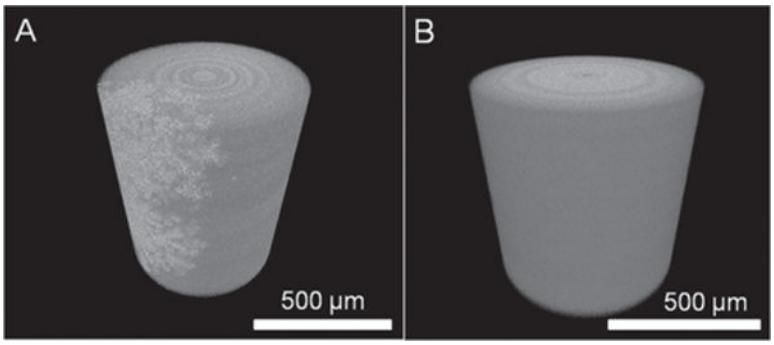

Figure 6.

3D images of the A) E1-50 and B) E2-50 adhesives cured under an LED light curing unit for 40s (LED Curebox, 200 mW cm^{-2} irradiance, Prototech, and Portland, OR). The morphologies were observed using 3D Micro XCT (Xradia Inc. Concord, CA).

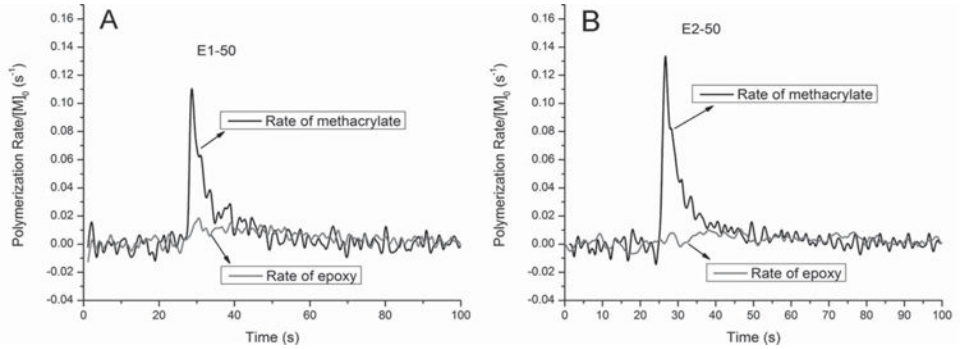

Figure 7.

Polymerization rate of methacrylates and ring-opening rate of epoxy groups versus time for A) E1- and B) E2-containing adhesive resins. A three-component initiator system was used: CQ/EDMAB/OPPIH = 1.0/1.0/2.0 (wt%). The adhesives were light-cured at room temperature using a commercial visible-light-curing unit (Spectrum 800, Dentsply, Milford, DE. Intensity was 550 mW cm^{-2}). E1-50: methacrylates/E1 = 50/50 (wt%); E2-50: methacrylates/E2 = 50/50 (wt%).

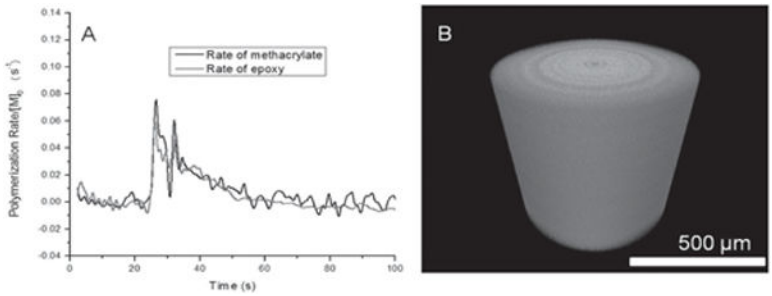

Figure 8.

A) Polymerization rate of methacrylates and ring-opening rate of epoxy groups versus time for E1-50-10 (weight content of E1 is 50 wt%; weight content of GBDA is 10 wt%). B) 3D images of the E1-50-10 adhesives cured under an LED light curing unit for 40s (LED Curebox, 200 mW cm^{-2} irradiance, Prototech, and Portland, OR). The morphologies were observed using 3D Micro XCT (Xradia Inc. Concord, CA).

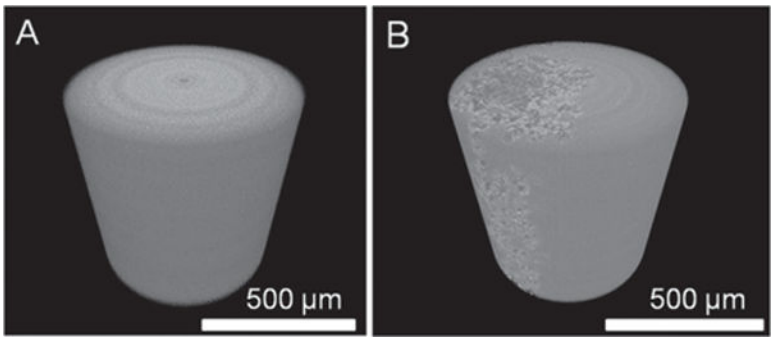

Figure 9.

3D images of the A) E1-25 (weight content of E1 is 25 wt%;) and B) E1-25-10 (weight content of E1 is 25 wt%; weight content of GBDA is 10 wt%) adhesives cured under an LED light curing unit for 40 s (LED Curebox, 200 mW cm^{-2} irradiance, Prototech, and Portland, OR). The morphologies were observed using 3D Micro XCT (Xradia Inc. Concord, CA).

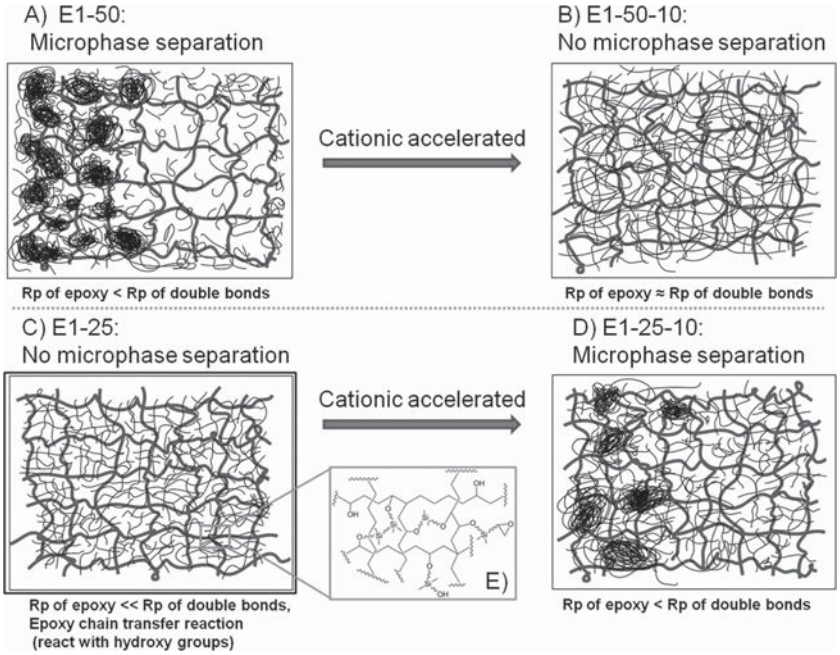

Figure 10.

Schematic illustration of microphase separation in free-radical/cationic ring-opening hybrid polymerization. The blue color represents chains of poly(methacrylate); the black color represents chains of siloxane-containing polymer. It should be noted that R_p is the ring-opening rate for the epoxy monomer, including the polymerization rate and the chain transfer rate.

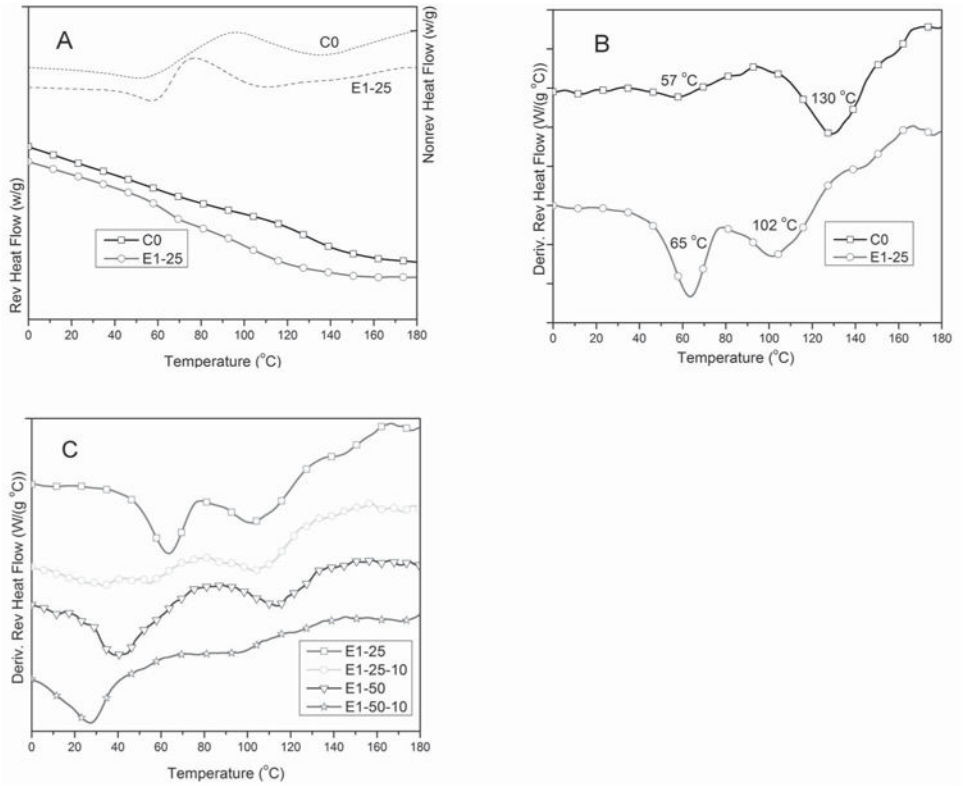

Figure 11.

Modulated DSC plots comparing C0 and E1-25 showing A) reversible heat flow, nonreversible heat flow, and B) derivative reversible heat flow. C) The derivative reversible heat flow for E1 with and without accelerator (GBDA).

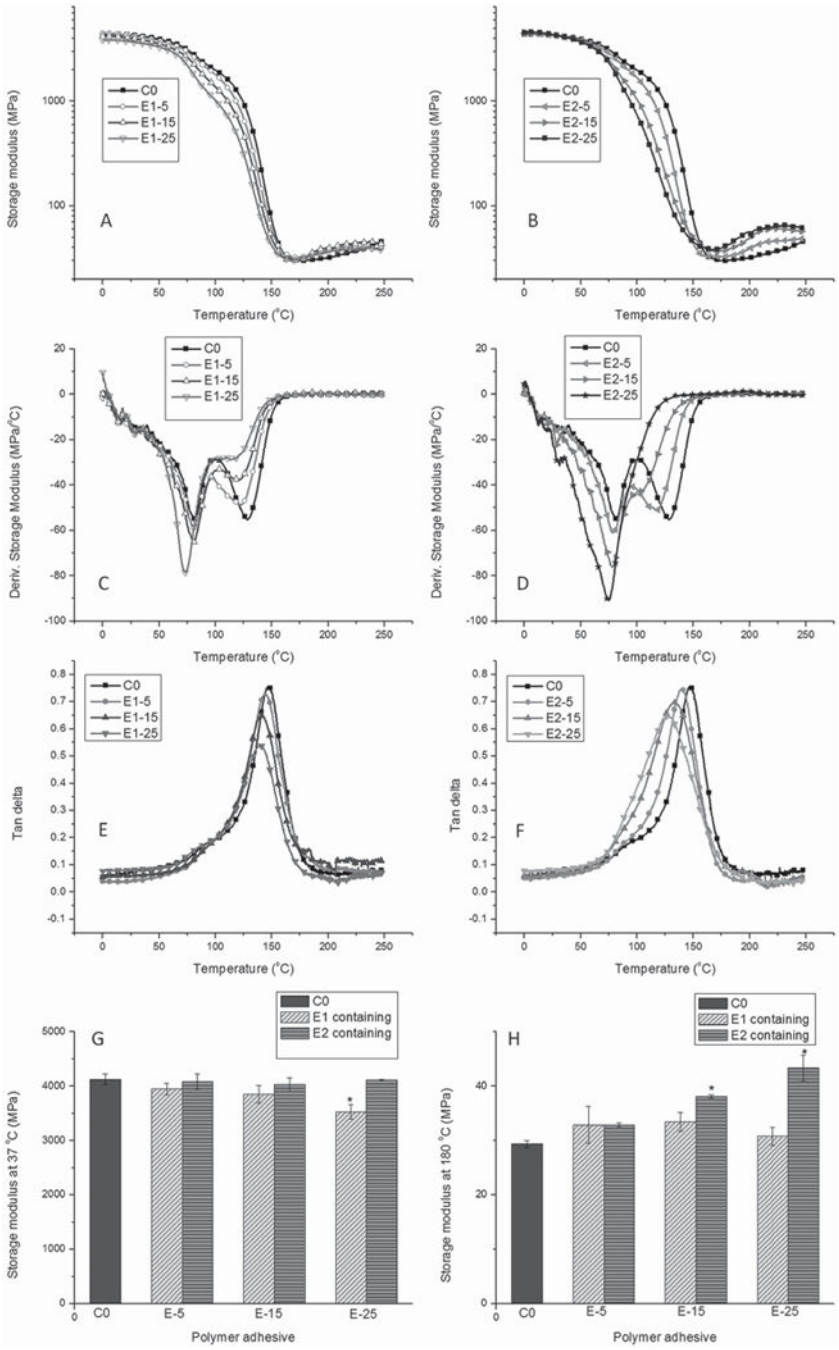

Figure 12.

DMA under dry conditions: Comparison of the storage modulus versus temperature curves for A) E1 and B) E2 and control formulations (C0). The derivative storage modulus versus temperature curves for the control and experimental formulations are shown in (C) and (D). Representative tan δ versus temperature curves for E) E1- and F) E2-containing polymers with different weight contents are shown. The intensity of the tan δ peak reflects the extent of mobility of polymer chain segments at this temperature. FWHM of the tan δ peak reflects the heterogeneity of the polymer networks. The comparison of storage modulus at 37 and

180 °C is shown in bar graphs of (G) and (H), respectively. Significantly ($p < 0.05$) different from the C0; Significantly ($p < 0.05$) different from the E-SM1. Symbols: E-*x*, *x* means the weight contents of epoxy monomer.

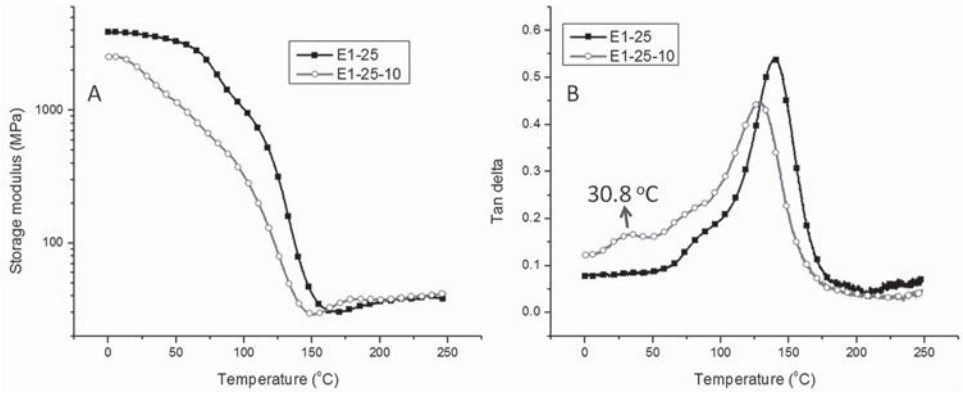

Figure 13.

A) Comparison of the storage modulus versus temperature curves for E1 formulations in the presence (E1-25-10, red curve) and absence (E1-25, black curve) of an accelerator (10% wt GBDA). B) Representative tan δ versus temperature curves for E1-25 and E1-25-10-containing polymers. DMA was done under dry conditions.

Table 1

Chemical structures used in the free-radical/cationic ring-opening hybrid system.

Initiator system		Monomer system	
Photosensitizer	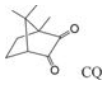 CQ	Methacrylate	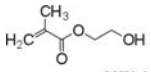 HEMA
Electron donor	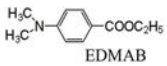 EDMAB		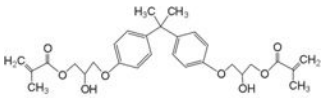 BisGMA
	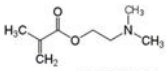 DMAEMA	Epoxide	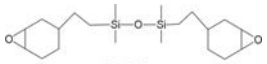 E1 (Siloxane epoxy)
Iodonium salt	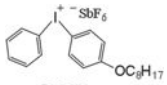 OPPIH		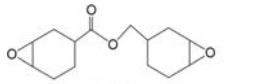 E2 (Oxocarbon epoxy)
Cationic ring-opening accelerator	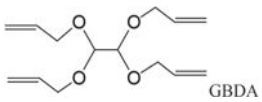 GBDA		

Table 2

Adhesive formulation, degree of conversion, and polymerization rate.

Photoinitiators (wt%) CQ/EDMAB/OPPIH	Sample[a)]	Methacrylates[b)] [wt%]	Epoxy [wt%]	Conversion of methacrylates [%][c)]	$R_p/[M]_0$ [s^{-1}]	Conversion of epoxy groups [%][c)]	Epoxy ring-opening rate/$[M]_0$ [s^{-1}]
0.5/0.5/1.0	C0	100	0	67.3 ± 0.3	0.27 ± 0.02		
	E1-5	95	5	71.4 ± 0.0[d)]	0.27 ± 0.03		
	E1-15	85	15	75.3 ± 0.0[d)]	0.21 ± 0.01[d)]		
	E1-25	75	25	76.1 ± 0.2[d)]	0.16 ± 0.02[d)]		
	E1-50	50	50	66.9 ± 1.3	0.13 ± 0.01[d)]	44.1 ± 1.4[e)]	0.02 ± 0.01[f)]
	E1-75	25	75	52.1 ± 1.1[d)]	0.07 ± 0.01[d)]	54.2 ± 0.2[e)]	0.02 ± 0.00[f)]
	E1-100		100			59.9 ± 0.4	0.06 ± 0.01
1.0/1.0/2.0	C0	100	0	69.8 ± 0.1	0.28 ± 0.01		
	E1-5	95	5	71.5 ± 0.0[d)]	0.24 ± 0.00[d)]		
	E1-15	85	15	72.2 ± 0.1[d)]	0.19 ± 0.02[d)]		
	E1-25	75	25	73.4 ± 0.0[d)]	0.16 ± 0.00[d)]		
	E1-50	50	50	68.9 ± 0.6	0.12 ± 0.01[d)]	68.0 ± 0.6[e)]	0.02 ± 0.00[f)]
	E1-75	25	75	58.7 ± 0.3[d)]	0.06 ± 0.00[d)]	65.5 ± 0.3	0.03 ± 0.00[f)]
	E1-100		100			65.8 ± 0.5	0.11 ± 0.01
	E1-25-10	65 + 10 (GBDA)[g)]	25	82.3 ± 2.1[d)]	0.12 ± 0.01[d)]		
	E1-50-10	40 + 10 (GBDA)[h)]	50	74.4 ± 0.7[d)]	0.08 ± 0.00[d)]	92.8 ± 0.3[e)]	0.06 ± 0.00[f)]
2.0/2.0/4.0	C0	100	0	74.2 ± 0.2	0.26 ± 0.02		
	E1-5	95	5	75.3 ± 0.2	0.22 ± 0.01[d)]		
	E1-15	85	15	75.6 ± 0.1	0.18 ± 0.01[d)]		
	E1-25	75	25	76.4 ± 0.1	0.18 ± 0.01[d)]		
	E1-50	50	50	73.9 ± 0.4	0.11 ± 0.01[d)]	62.0 ± 0.2[e)]	0.03 ± 0.00[f)]
	E1-75	25	75	65.4 ± 2.8[d)]	0.08 ± 0.01[d)]	64.3 ± 0.0[e)]	0.05 ± 0.00[f)]
	E1-100		100			68.0 ± 0.5	0.10 ± 0.01
1.0/1.0/2.0	E2-5	95	5	72.5 ± 0.7	0.26 ± 0.00		

Photoinitiators (wt%) CQ/EDMAB/OPPIH	Sample[a)]	Methacrylates[b)] [wt%]	Epoxy [wt%]	Conversion of methacrylates [%][c)]	$R_p/[M]_0$ [s^{-1}]	Conversion of epoxy groups [%][c)]	Epoxy ring-opening rate/$[M]_0$ [s^{-1}]
	E2-15	85	15	76.6 ± 0.3[d)]	0.23 ± 0.01[d)]		
	E2-25	75	25	79.7 ± 0.2[d)]	0.18 ± 0.01[d)]		
	E2-50	50	50	79.3 ± 0.0[d)]	0.15 ± 0.00[d)]	40.1 ± 0.1[i,j)]	0.01 ± 0.00[j)]
	E2-75	25	75	77.7 ± 1.4[d)]	0.08 ± 0.01[d)]	37.9 ± 0.5[i,j)]	0.02 ± 0.00[j)]
	E2-100		100			36.2 ± 2.7[i,j)]	0.05 ± 0.01[j)]

[a)] E1: E1-containing adhesives; E2: E2-containing adhesives; E*N*-*x*: *x* is the weight content of epoxy monomer;

[b)] Methacrylates: HEMA/BisGMA = 45/55;

[c)] The values of degree of conversion were obtained from the intensity of FTIR spectra changing after 10 min recording;

[d)] Significant ($p < 0.05$) difference from Control C0 with the same content of photoinitiators;

[e)] Significant ($p < 0.05$) difference from E1-100 with the same content of photoinitiators;

[f)] Significant ($p < 0.05$) difference from E1-100 with the same content of photoinitiators;

[g)] Methacrylates: 65 wt% (HEMA/BisGMA = 45/55); GBDA: 10 wt%;

[h)] Methacrylates: 40 wt% (HEMA/BisGMA = 45/55); GBDA: 10 wt%;

[i)] Degree of conversion of E2 was calculated by monitoring the decrease of peak intensity of epoxy groups at 788 cm^{-1} in the FTIR spectra;

[j)] Significant ($p < 0.05$) difference from E1-containing formulations with the same content of epoxy and with the same content of photoinitiators. Values are mean (± standard deviation) for $n = 3$ in each group.

Table 3

DMA data for control and experimental adhesives under dry conditions.

Sample	Storage modulus at 25 °C [MPa]	Storage modulus at 37 °C [MPa]	Storage modulus at 180 °C [MPa]	T_g [°C][a)]	Height of tan δ peak	FWHM values of tan δ peak [°C][b)]
C0	4301 ± 102	4125 ± 95	29.37 ± 0.68	147.29 ± 0.57	0.74 ± 0.02	35.58 ± 1.74
E1-5	4138 ± 122	3948 ± 108	32.88 ± 3.43	142.91 ± 1.52[c)]	0.72 ± 0.02	42.79 ± 1.59[c)]
E1-15	4031 ± 173	3852 ± 158	33.43 ± 1.71	142.59 ± 0.76[c)]	0.68 ± 0.03[c)]	42.76 ± 1.97[c)]
E1-25	3697 ± 149[c)]	3526 ± 129[c)]	30.79 ± 1.69	139.77 ± 0.90[c)]	0.57 ± 0.03[c)]	43.69 ± 2.27[c)]
E1-25-10	1816 ± 148[c)]	1381 ± 106[c)]	38.22 ± 0.88[c)]	128.31 ± 0.01[c)]	0.46 ± 0.02[c)]	55.83 ± 3.42[c)]
E2-5	4269 ± 18	4083 ± 145	32.87 ± 0.36	139.10 ± 0.86[c)]	0.73 ± 0.02	41.07 ± 1.39[c)]
E2-15	4265 ± 105	4030 ± 127	38.12 ± 0.28[c)]	134.18 ± 1.53[c)]	0.69 ± 0.01[c)]	53.02 ± 1.63[c)]
E2-25	4386 ± 56	4111 ± 10	43.31 ± 2.35[c)]	127.90 ± 0.80[c)]	0.65 ± 0.01[c)]	54.31 ± 5.20[c)]

[a)] The T_g values of the polymer networks were taken to be the maximum of the tan δ versus temperature curve, which was determined by using a dynamic mechanical analyzer. T_g from DMA was higher than that got from DSC study due to the different signal responds with different technique;

[b)] FWHM values of tan δ peak were analyzed by Gauss fit (Fit single peak) using Microcal Origin Version 8.0 (Microcal Software Inc., Northampton, MA);

[c)] Significant ($p < 0.05$) difference from Control C0. Values are mean (± standard deviation) for $n = 3$ in each group.